RESEARCH ARTICLE

Key Points:
- Plate rotation during collision can assist in the exhumation of UHP terranes
- Plate rotation helps explain the discontinuous distribution of UHP terranes
- Numerical modeling fits with observations from the Western Gneiss Norway

Supporting Information:
- Read_Me
- Figures S1–S12.
- suppinfo ms01–ms02.
- Appendix_2__review_final

Correspondence to:
A. D. Bottrill,
a.d.bottrill@durham.ac.uk

Plate rotation during continental collision and its relationship with the exhumation of UHP metamorphic terranes: Application to the Norwegian Caledonides

A. D. Bottrill[1], J. van Hunen[1], S. J. Cuthbert[2], H. K. Brueckner[3], and M. B. Allen[1]

[1]Department of Earth Sciences, Durham University, Durham, UK, [2]School of Science, University of the West of Scotland, Paisley, UK, [3]Lamont-Doherty Earth Observatory of Columbia University, Palisades, New York, USA

Abstract Lateral variation and asynchronous onset of collision during the convergence of continents can significantly affect the burial and exhumation of subducted continental crust. Here we use 3-D numerical models for continental collision to discuss how deep burial and exhumation of high and ultrahigh pressure metamorphic (HP/UHP) rocks are enhanced by diachronous collision and the resulting rotation of the colliding plates. Rotation during collision locally favors eduction, the inversion of the subduction, and may explain the discontinuous distribution of ultra-high pressure (UHP) terranes along collision zones. For example, the terminal (Scandian) collision of Baltica and Laurentia, which formed the Scandinavian Caledonides, resulted in the exhumation of only one large HP/UHP terrane, the Western Gneiss Complex (WGC), near the southern end of the collision zone. Rotation of the subducting Baltica plate during collision may provide an explanation for this distribution. We explore this hypothesis by comparing orthogonal and diachronous collision models and conclude that a diachronous collision can transport continental material up to 60 km deeper, and heat material up to 300°C hotter, than an orthogonal collision. Our diachronous collision model predicts that subducted continental margin material returns to the surface only in the region where collision initiated. The diachronous collision model is consistent with petrological and geochonological observations from the WGC and makes predictions for the general evolution of the Scandinavian Caledonides. We propose the collision between Laurentia and Baltica started at the southern end of the collisional zone, and propagated northward. This asymmetric geometry resulted in the counter clockwise rotation of Baltica with respect to Laurentia, consistent with paleomagnetic data from other studies. Our model may have applications to other orogens with regional UHP terranes, such as the Dabie Shan and Papua New Guinea cases, where block rotation during exhumation has also been recorded.

1. Introduction

The study of high pressure/ultra-high pressure (HP/UHP) metamorphic rocks is important as these rocks offer an insight into lithospheric conditions as well as providing useful constraints on the continental collision process [*Dobrzhinetskaya et al.*, 2011b; *Warren*, 2013]. Exhumed HP/UHP rocks are present in most Phanerozoic collision zones [*Dobrzhinetskaya et al.*, 2011a] and probably resulted from the subduction of one continental margin beneath another, but their exhumation mechanisms and resultant structures vary. A number of different mechanisms have been proposed for the return of HP/UHP rocks to the surface, ranging from whole scale return of the subducted plate to exhumation of small supracrustal slivers [*Kylander-Clark et al.*, 2012]. Numerical modeling work by *Burov et al.* [2001] shows how return flows generated in the subduction channel can return subducted continental crust to the surface. Others have shown how exhumation can occur when the buoyancy of subducted continental crust exceeds the shear traction exerted on it by its underlying lithosphere [*Warren et al.*, 2008a], resulting in its return toward the surface as a coherent slab. Furthermore, "eduction" has been proposed [*Dixon and Farrar*, 1980; *Andersen et al.*, 1991] where the subduction trajectory is completely reversed, bringing the whole plate (crust and lithosphere) back to the surface. The need for different exhumation mechanisms is a reflection on the variety in size and structure of UHP terranes [*Kylander-Clark et al.*, 2012].

This study focuses on eduction as a mechanism for returning HP/UHP metamorphic terranes to the surface (we follow the convention that UHP rocks are those that have equilibrated at pressures above the minimum stability of coesite; some such rocks are known to have formed at pressures well into the P-T stability field

of diamond—see *Dobrzhinetskaya et al.* [2011b]). The force balance for the reversal of plate motion is explored by *Duretz et al.* [2012] who show that slab breakoff removes the slab pull force allowing the partially subducted buoyant continental plate to return back up along the original subduction trajectory. This bulk movement of the partially subducted continental block and its underlying mantle lithosphere back along the original subduction path reverses the shear sense on the upper subduction interface and has the potential of exhuming large quantities of continental material in one coherent section. This mechanism is favored for large terranes as it explains both the size and structural coherence of exhumed crustal material. An example of a large HP/UHP terranes is the Norwegian Western Gneiss Complex (WGC) in the southern Scandinavian Caledonides [*Andersen et al.*, 1991; *Teyssier*, 2011; *Brueckner and Cuthbert*, 2013].

The Western Gneiss Complex (WGC) is one of the largest exposed HP/UHP terranes currently preserved on earth. It formed during the terminal Caledonian collision between the continents Laurentia and Baltica. This collision, known as the Scandian Orogeny, occurred in the Silurian [*Dewey and Strachan*, 2003]. The collision dynamics are complicated by the earlier collisions of a number of continental and island arc fragments [*Brueckner and van Roermund*, 2004] but paleomagnetic evidence suggests the final collision started in the south then closed progressively toward the north [*Torsvik et al.*, 2012]. The WGC is considered to represent the continental margin of Baltica that underwent deep but transient subduction beneath Laurentia during collision, followed by wholesale exhumation [*Hacker and Gans*, 2005; *Hacker*, 2007; *Brueckner and Cuthbert*, 2013] a map of the major tectono/stratigrapic units and structures is provided in supporting information (Figure Siii) adapted from [*Brueckner and Cuthbert*, 2013].

The metamorphism recorded in the WGC shows a progression in metamorphic grade, from ultra-high pressures recorded in the northwest to weakly metamorphosed in the southeast [*Hacker et al.*, 2010]. The pressures experienced by the westernmost portion of this terrane are thought to have been particularly high as some lithologies contain coesite [*Smith*, 1984; *Wain*, 1997; *Cuthbert et al.*, 2000; *Terry et al.*, 2000; *Walsh and Hacker*, 2004; *Butler et al.*, 2013] and microdiamonds [*Dobrzhinetskaya et al.*, 1995; *van Roermund et al.*, 2002; *Vrijmoed et al.*, 2006], which are consistent with thermobarometric estimates of pressure temperature (P-T) conditions of up to 5 GPa and 900°C [*Cuthbert et al.*, 2000; *Terry et al.*, 2000; *Carswell et al.*, 2006; *Vrijmoed et al.*, 2006] and indicate subduction of continental crust to depths of as much as 165 km. This progression in metamorphic grade has been interpreted as evidence that Baltica was subducted northwestward (present coordinates) beneath Laurentia [*Krogh*, 1977; *Griffin et al.*, 1985; *Hacker et al.*, 2010], metamorphosed under HP/UHP conditions, and then returned, as the WGC, to the surface as one quasi-coherent unit [*Andersen et al.*, 1991; *Wilks and Cuthbert*, 1994; *Brueckner*, 2006; *Warren et al.*, 2008b]. The timing of collision and continental subduction in the southern Norwegian Caledonides is constrained by the development of a clastic fill in a foredeep basin during Ludlow to Pridoli times, from 427 to 419 Ma [*Davies et al.*, 2005], by early eclogite development in the associated Lindås Nappe at ∼430 Ma [*Glodny et al.*, 2008], and by the older ages obtained from UHP eclogites and garnet pyroxenites in the WGC at around 434–425 Ma [*Kylander-Clark et al.*, 2007; *Spengler et al.*, 2009], which probably document subduction after initial collision. Collision is unlikely to have initiated earlier than 434.0 ± 3.9 Ma, the age of a pre or syncollisional granite intruded into an ophiolite/arc unit in the Upper Allochthon [*Hacker et al.*, 2003]. WGC eclogite mineral ages continue to range down to about 400 Ma, with a few as young as 370 Ma, indicating that parts of the WGC remained at mantle depths until at least that time [*Kylander-Clark et al.*, 2009]. A review of the age patterns in the WGC as well as evidence for the reversal of shear sense between the allochthons and the WGC suggests the transition from subduction to eduction occurred at ∼405 Ma [*Brueckner and Cuthbert*, 2013 and references therein].

The WGC outcrops within a very large tectonic window and is separated by a major shear zone from two overlying thrust-nappe complexes, the Jotun nappe complex of the Middle Allochthon, and the Trondheim nappe complex of the Upper Allochthon, which outcrop to the east and southeast of the WGC, respectively, and which have further equivalents in the western coastal region (supporting information Figure Siii) [*Hacker and Gans*, 2005; *Andersen and Austrheim*, 2008; *Milnes and Corfu*, 2008; *Gee et al.*, 2010]. These allochthons comprise the Scandian orogenic wedge created during the early phases of Caledonian (Scandian) Laurentia-Baltica collision. *Brueckner and Cuthbert* [2013] have recently argued that this orogenic wedge was ruptured during the reversal of shear sense between the WGC and the allochthons, and the Jotun and Trondheim Nappe Complexes were then further transported piggy-back on top of the educting WGC to their current position. This deformation of the wedge was argued to have also resulted in the formation on

the Devonian intramontane basins that lie along the west coast of southern Norway. As noted above, motion reversal in the subduction channel and the initiation of eduction is thought to have happened at about 405 Ma [*Brueckner and Cuthbert*, 2013] after which the WGC cooled to Ar^{40}-Ar^{39} closure temperatures of white mica by 397–380 Ma [*Walsh et al.*, 2013]. The youngest Ar-Ar ages are broadly coincident with depositional ages in the intramontane basins [*Wilks and Cuthbert*, 1994]. Final exhumation of the WGC is not well constrained as no detritus from it is recognizable in the intramontane basins [*Cuthbert et al.*, 1983], but the most deeply subducted material now at outcrop had reached normal midcrustal depths by about 380 Ma, giving a total interval of ~50 Ma from collision to the approximate end of eduction.

Ar-Ar cooling ages for the WGC are 20 Myr older in the southeast portion of its outcrop area than in the northwest [*Walsh et al.*, 2013] suggesting again that exhumation occurred progressively from southeast to northwest, which is consistent with eduction toward the south-east. The process of whole-lithosphere eduction as an exhumation mechanism for the WGC remains controversial; for example, exhumation as a giant flake or nappe up to 14 km thick has been proposed [*Carswell et al.*, 2003], but to date no convincing basal thrust to accommodate transport of such a large mass has been discovered. The presence of basement-involved eclogite-bearing allochthons such as the Lindås nappe [*Glodny et al.*, 2008] and the upper basement unit in the Trollheimen-Moldefjord region [*Robinson*, 1995] undoubtedly indicate that the Baltica margin underwent at least superficial imbrication during the early stages of its subduction, hence some crustal flakes or nappes may have exhumed by extrusion along the subduction channel. However, this cannot explain the exhumation of the remaining, much larger, structurally underlying mass of the HP WGC. Hence, in the absence of convincing evidence for a basal thrust zone, we prefer a mechanism involving wholesale withdrawal (eduction) of the Baltica margin from the subduction channel while still attached to the rest of the Baltic craton as well as the underlying lithosphere.

Exhumation by eduction relies on a change in the force acting on the subducting continental margin. One way to achieve this is the breaking off of the dense oceanic slab to allow the buoyant continental block to exhume. Slab breakoff has been proposed as one of the final stages of continental collision [*Davies and von Blanckenburg*, 1995], and imaged with tomography for a number of collision zones [*Nolet*, 2009], as well as being inferred from earthquake gaps [*Roecker*, 1982]. Slab breakoff may also be regarded as the trigger for exhumation as a result of the release of "slab pull." Slab breakoff probably occurs by lateral tearing along the subducted slab [*Yoshioka et al.*, 1995; *Wortel & Spakman*, 2000; *Van Hunen and Allen*, 2011] and is suggested to be responsible for topographic depressions that propagate along collision zones [*Van der Meulen et al.*, 1998; *Sperner et al.*, 2001]. Slab tearing has been shown to start where collision first occurred [*Van Hunen and Allen*, 2011]. The force balance for the continental collision and slab breakoff [*Duretz et al.*, 2012] is influenced by the buoyancy of the partially subducted continental plate which will cause return of subducted material once the slab pull force has been removed. If the subducted continental material remains strong and coherent, this return will take the form of wholesale plate eduction. Far field forces that act on the subduction system also need to be considered as they could assist in the eduction process [*Fossen*, 2010; *Brueckner and Cuthbert*, 2013]. Considering the likelihood of the propagation of breakoff along the collision zone, we expect there would also be variation in timing and amount of material exhumation along the collision zone. The exact nature of the Iapetus subduction system and slab detachment between Laurentia and Baltica is still debated [*Andreasson et al.*, 2003; *Fossen*, 2010] though the majority of evidence suggests a westward subduction of Baltic under Laurentia.

Here we examine numerically the exhumation of HP/UHP rocks after collision; subduction and slab breakoff, and investigate the differences in exhumation patterns produced by diachronous versus orthogonal collisions. We present two 3-D dynamic numerical models of the closure of an oceanic basin; a first where collision occurs all along the collision zone at the same time (orthogonal collision), and a second where collision initiates at one end and propagates along the collision system (diachronous collision). These models are then compared to pressure, temperature, and time (P-T-t) estimates from the WGC.

2. Methodology

To assess the role of a diachronous collision and associated plate rotation on the exhumation of UHP terranes we developed 3-D numerical flow models of continental collision and slab breakoff. Synthetic pressure-temperature-time (P-T-t) paths are calculated so that they can be compared to field observations.
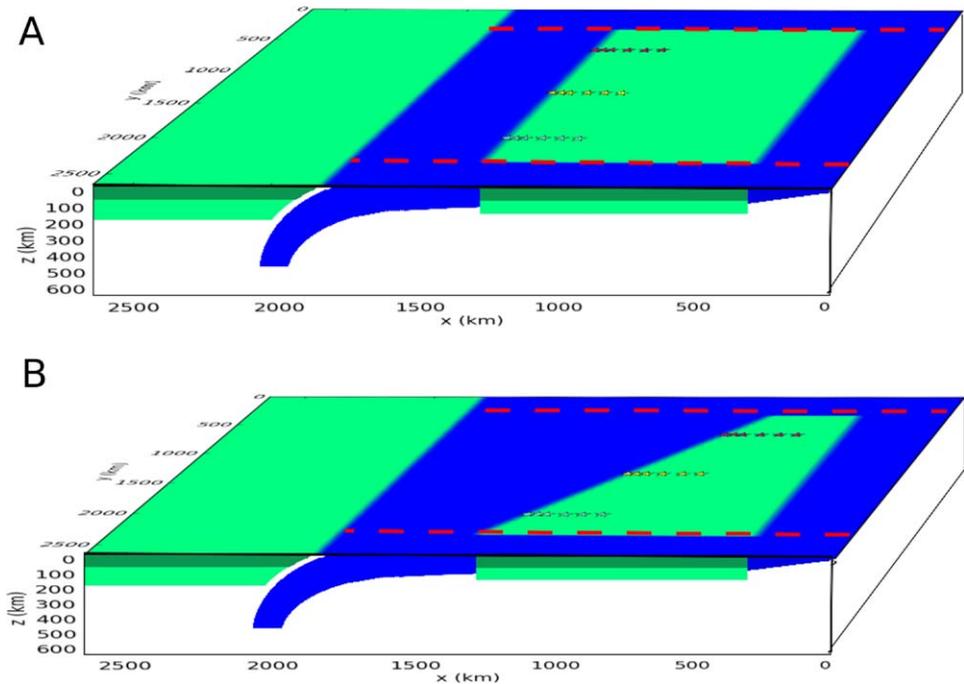
Figure 1. Schematic 3-D model setup for the collision models. Models have a computational domain size of 2640 km by 2640 km by 660 km. Both models have a 20 km weak zone and 100 km × 66 km mantle wedge that decouple the two plates. Two transform faults (red-dashed lines) cut the subducting plate and decouple it from the model boundaries. The models differ in the shape of the continental block embedded in the subducting plate: (a) A rectangular continental block and will be referred to as the orthogonal collision model. (b) A trapezoid shaped continental block and shall be referred to as the diachronous collision model. Each of the three sets of six stars represents a family of material markers placed at y = 660, 1320, and 1980 km. Each family contains 24 markers placed in a 6 × 4 grid in the x-z plane. An example of the position of the markers for one family in x and z directions is shown in Figure 2.

The numerical model uses a Cartesian, incompressible-flow version of the finite element geodynamical code Citcom [*Moresi and Gurnis*, 1996; *Zhong et al.*, 2000; *van Hunen and Allen*, 2011]. In the model setup, we adopt the Boussinesq approximations. Conservation of mass, momentum, energy, and composition are applied using the following nondimensional governing equations:

$$\nabla \cdot \overrightarrow{u} = 0 \tag{1}$$

$$-\nabla P + \nabla \cdot \left(\eta \left(\nabla \overrightarrow{u} + \nabla \overrightarrow{u}^{T} \right) \right) + (RaT + RbC)\hat{e}_z = 0 \tag{2}$$

$$\frac{\partial T}{\partial t} + \overrightarrow{u} \cdot \nabla T = \nabla^2 T \tag{3}$$

$$\frac{\partial C}{\partial t} + \overrightarrow{u} \cdot \nabla C = 0 \tag{4}$$

where $\overrightarrow{u}$ is the velocity, P is the deviatoric pressure, η the viscosity, Ra the thermal Rayleigh number, Rb the compositional Rayleigh number, $\hat{e}_z$ the vertical unit vector, C a material parameter that distinguishes crust from mantle material, T the temperature, and t is time.

In this setup, flow of material is driven by combined thermal and compositional buoyancy. The continental material is advected, in accordance with Equation (4), using particle tracers [*Di Giuseppe et al.*, 2008]. These tracers are also used as passive markers to monitor the P-T-t path of individual pieces of the continental plate that enter the subduction zone.

The models in this study simulate the closure of an oceanic basin leading to continental collision, partial subduction of continental material, slab detachment and subsequent exhumation. The two initial model setups investigated are shown in Figure 1. The computational domain is 660 km by 2640 km by 2640 km giving a 4:4:1 aspect ratio in x, y, z, where the x direction is perpendicular to the collision zone, and the
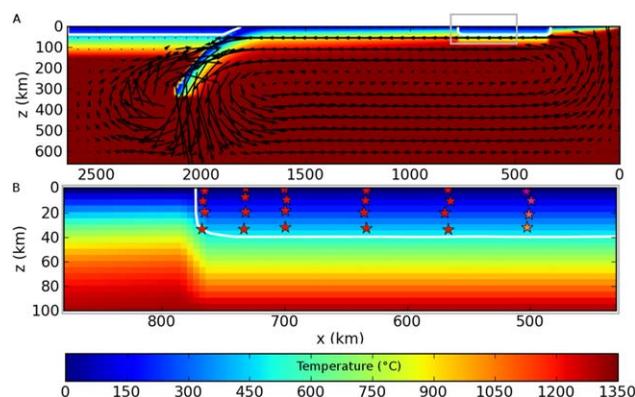
Figure 2. (a) Initial temperature distribution and velocity vectors at t = 0. (b) Zoom-in of gray rectangle in A showing the initial positions of one family of markers within the continental crust of the subducting plate. White contour lines outline the continental crust. Markers are initially placed at depths of 0, 10, 20, and 30 km, and at distances of 0, 30, 60, 120, 180, and 240 km from the front of the continental block.

y direction is parallel to the collision zone, and the *z* direction is downward. The models use a nondeformable Cartesian grid with a high resolution region in the top 200 km and between *x* = 1700 km and *x* = 2200 km over the collision zone. This gives a grid resolution, over the collision zone, of 10 km by 20 km by 10 km in the *x*, *y*, *z* directions, respectively (see Figures Si and Sii in supporting information for a representative cross section through the grid and results of a resolution test, respectively).

Flow boundary conditions for the model are free-slip on the top and sides and no-slip on the base. These boundary conditions do not allow any flow through the model boundaries. This means that all forces that drive subduction, such as slab pull, are generated internally in the model. The no-slip boundary condition at the base of the model is designed to simulate the interaction of a slab with a higher viscosity lower mantle. The thermal boundary conditions are 0°C at the surface and a mantle temperature of 1350°C at the base of the model domain and *x* = 0 boundary. Keeping the *x* = 0 boundary at mantle temperature simulates a mid-ocean ridge. The other three sides have a zero heat flux boundary condition.

Subduction is initiated by a 400 km hanging oceanic slab sinking into the mantle and facilitated by a 20 km wide zone of weak material between the subducting plate and the overriding plate, as well as a 100 km high and 66 km wide weak mantle wedge. The weak zones are sustained throughout the model calculations and kept at a relatively low viscosity (10^{20} Pa·s) to allow permanent decoupling of the two plates. The model setup initially has a 60 Myr old oceanic lithosphere subducting to the left under a continental overriding plate. In the *y* direction (trench parallel), the 1980 km slab is bounded at *y* = 330 and 2310 by two 20 km wide weak zones (viscosity 10^{20} Pa s) that serve as transform faults (Figure 1). The initial thermal structure (Figure 2) of the oceanic lithosphere is calculated using the half space cooling model, which converts a lithosphere age to a thickness. There is a linear increase in oceanic plate age from 0 Myr at the right edge to 60 Myr at the trench. A thicker, lower density continental block is embedded in the subducting plate with a linear geotherm from 0°C at the surface to mantle temperature of 1350°C at 100 km. The thermal structure of the still thicker overriding continental plate is set as a linear geotherm from 0°C at the surface to mantle temperature at 150 km. The thicker lithosphere of the overriding plate is designed to simulate the collision of a smaller continent with a larger cratonic continent.

The 40 km thick continental crust in the model resists subduction due its compositional buoyancy of 600 kg/m^3. Oceanic crustal buoyancy is ignored in the models, as the assumed transformation of basalt to eclogite of oceanic crust would remove any initial compositional buoyancy [*Cloos*, 1993]. The transformation to denser rock types such as eclogite within the continental crust would also have an influence on the buoyancy of continental material that is transported to depth. Large HP/UHP terranes such as in the WGC in Norway do indeed contain dense eclogitic rocks but generally eclogite makes up a low percentage of the total rock [*Cuthbert et al.*, 2000]. The limited evidence available from felsic rocks that have escaped the pervasive retrogressive metamorphic overprint indicates that transformation of the dominant granitoid orthogneisses to dense UHP mineral assemblages was very limited [*Carswell et al.*, 2003]. Therefore, for buoyancy purposes, we ignore the complexity of possible phase changes in the continental crust, and assume that, on average, the material that currently makes up terranes such as the WGC lack sufficient dense lithologies to substantially influence the average crustal density.

To investigate possible reasons for differences in the exhumation processes along the collision zone such as those proposed by *Fossen* [2010] and *Zhang et al.* [2009], we compare two end-member models, one with a

rectangular-shaped continental block (Figure 1a) and the other with a trapezoid-shaped continental block (Figure 1b). The rectangular continental block is 1000 km long along both the transform faults, and thus represents an orthogonal collision. The trapezoid shaped continental block is 500 km long along the $y = 330$ km transform fault and 1000 km long along the $y = 2310$ km transform fault. This geometry was chosen as it generates a diachronous collision that propagates along the full length (1980 km) of the subduction zone in ∼20 Myr. The diachronous collision also creates a rotation of the subducting plate, thereby assisting eduction at one end of the subduction zone. The continental block extends over the full 1980 km width between the two transform faults in both models. The overriding plate does not move in the reference frame of the model, extends over the full model width in the y direction and has a 40 km thick continental crust and a lithosphere that extends down to 150 km.

The strength of the material in our model is governed by temperature and stress-dependent rheology. Four different deformation mechanisms are used: (1) diffusion creep, (2) dislocation creep [*Karato and Wu*, 1993], (3) a stress limiting rheology [*Byerlee*, 1978], which weakens material near the surface when under high stresses, and (4) a model maximum viscosity for numerical stability. A more detailed description of the applied rheology is presented in [*Van Hunen and Allen*, 2011; *Bottrill et al.*, 2012].

Three families of material markers are placed in the frontal portion of the subducting continental block at $y = 660$ km (red stars), $y = 1320$ km (yellow stars) and $y = 1980$ km (blue stars), and are followed to calculate P-T-t paths (Figures 1 and 2). The 1320 km marker-set is in the center of the continental block whereas the 660 and 1980 km marker-sets are 330 km inward from the two edges of the continental block. Each family contains 24 material markers that are placed in a 6 × 4 grid in the *x-z* plane with markers at depths of 0, 10, 20, and 30 km and at distances of 0, 30, 60, 120, 180, and 240 km from the front of the continental block (Figure 2b). When calculating the P-T-t path for the marker, we add an additional vertical thermal gradient $dT/dz = 0.5$ °C/km to account for adiabatic heating. We define the $y = 0$ edge of the model as the "north" edge and the $y = 2640$ km as the "south" edge.

Maximum horizontal eduction distances are calculated for each family of markers. Only the markers furthest from the front of the continental block (i.e., 240 km from the front) are used as they only just reach the subduction zone and so have almost no vertical component to their motion. The maximum eduction distance is defined as the maximum horizontal return distance, as measured along the *x* axis of the model.

3. Results

We first present the dynamics, exhumation patterns, and P-T-t paths for the orthogonal collision model, which we then compare with results from the diachronous collision model. For simplicity, we only present results for one family of material markers in each model (the middle family at $y = 1320$ km for the orthogonal collision and the family at $y = 1980$ km for the diachronous collision). Full results for all material markers for both models are presented in the supporting information.

3.1. Orthogonal Collision

The dynamics of an orthogonal collision mode are presented for $y = 1320$ km in cross section (left side) and for all three families of markers in plan view (right-hand side) in Figure 3. The model shows a slowing of the subduction velocity (represented by the lengths of the velocity arrows in Figures 3e and 3f) after collision, when continental material starts to be subducted. At t = 20 Myr, slab breakoff detaches the dense oceanic lithosphere from the buoyant continental block, and changes the average buoyancy of the subducted plate. The partially subducted continental plate therefore returns back toward the surface along the original subduction path (reversed arrows in Figure 3g). This velocity reversal is shown within the slices through the modeling domain (Figures 3c and 3d) by the movement of the material markers back up the along their original subduction path after slab breakoff.

The material markers indicate the movement of the continental crust during collision, subduction, and exhumation. Some of the surface markers are accreted onto the base of the overriding plate during the continental subduction. However, the deeper markers, positioned initially at 10–30 km, are transported to depth along with the front portion of the continental plate. After slab breakoff, these markers move backward, out of the subduction zone, together with the rest of the subducted lithosphere. Figures 3a–3d shows that markers that started furthest from the trench are still orientated in the same grid pattern as they
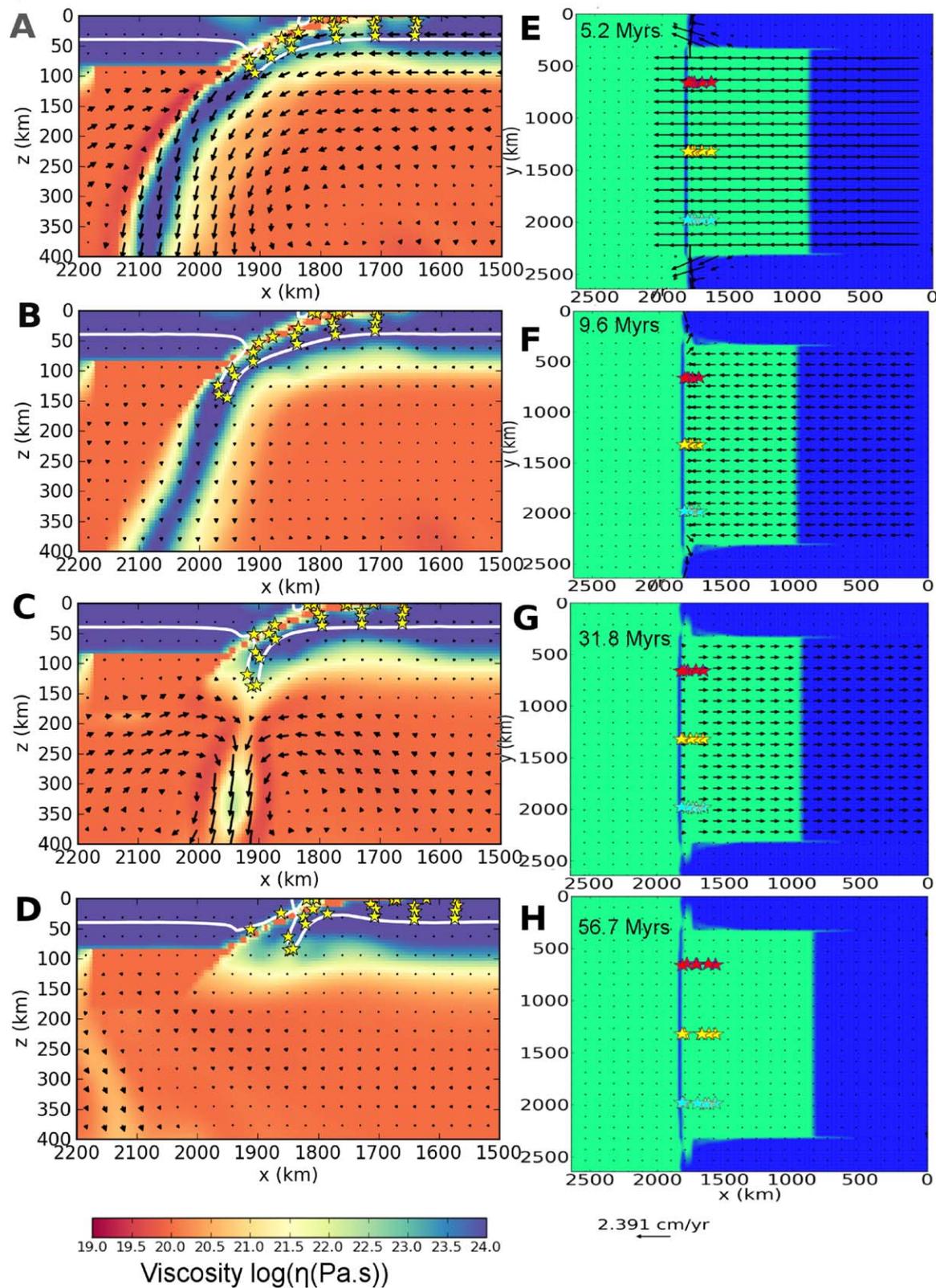
Figure 3. (a–d) Time slices through the center of the orthogonal collision model, with time increasing from Figures 3a to 3d. Color scheme shows viscosity variations, the white contour highlights crustal material and stars show the positions of followed material markers. (e–h) Time snapshots of surface velocity (green = continental material, blue = oceanic material). The stars represent surface markers. Time increases from Figures 3e to 3h.
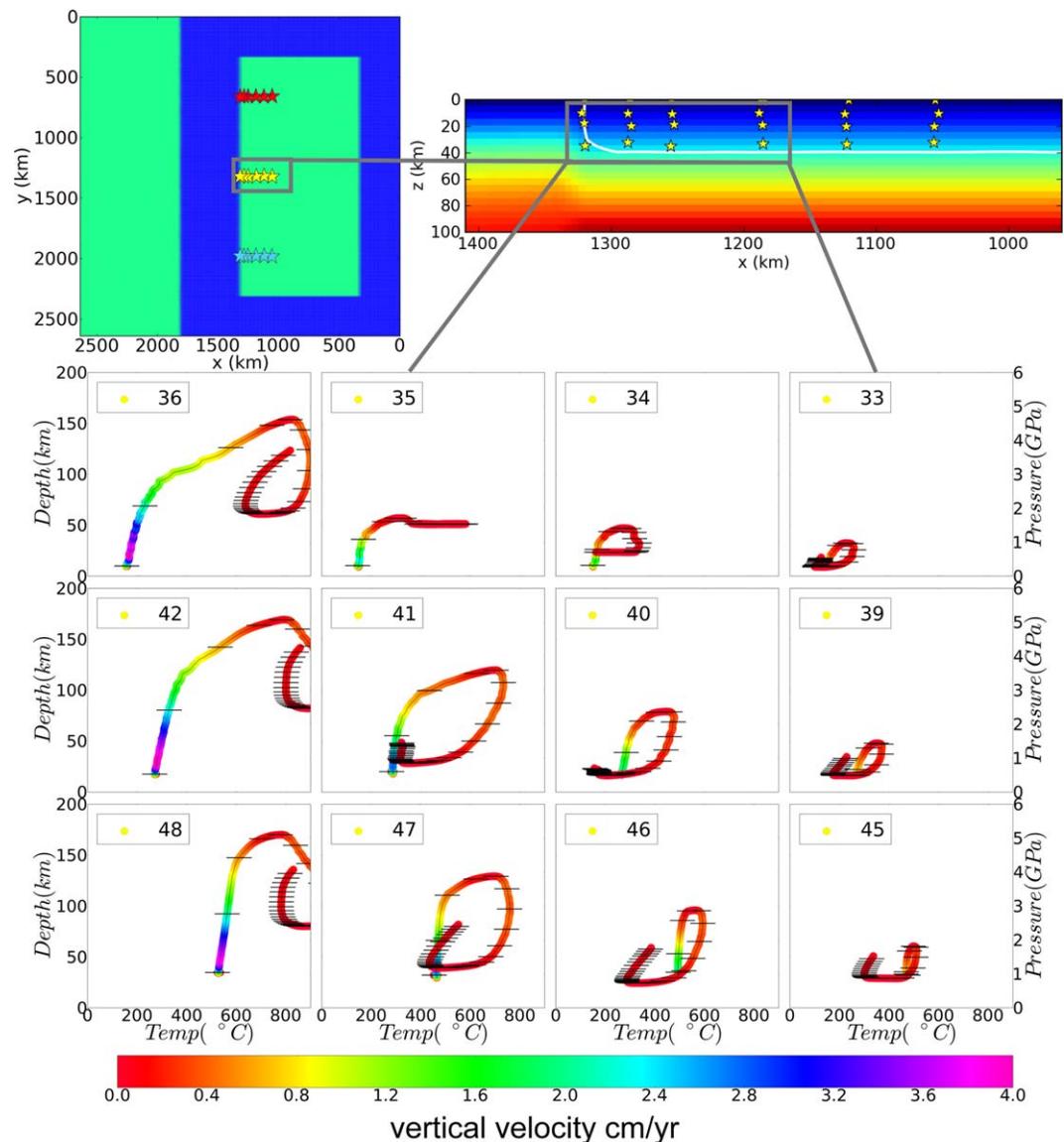
Figure 4. P-T-t (pressure temperature time) paths for material markers that started in the center of the orthogonal collision model and were placed, from top to bottom, at 10, 20, and 30 km depth and, from left to right at 0, 30, 60, and 120 km form the front of the subducting continental block. The shown configuration of P-T-t paths represents the grid in which the markers where originally arranged at the start of the model. The number in the top left of the plot is the markers unique number. The colors of each P-T-t path show the vertical velocity of the material markers. The distances between the black horizontal bars across the paths represent a time period of 5 Myr.

started with after eduction. The markers in the front portion of the plate experience some reorganization but generally the continental plate was coherently subducted and then educed as shown by the white contour that outlines the crustal material. The orthogonal model has a horizontal eduction distance of 156 km along the whole length of the collision zone.

P-T-t paths are presented in Figure 4 for the material markers from the family of markers that started in the center of the model domain (yellow stars at $y = 1320$ km in Figures 1 and 3) and were initially positioned between depths of 10–30 km and at distances 0–120 km from the front of the subducting continental block. P-T paths for all markers from all three families are presented in the supporting information. Similarly positioned markers from the two other families show almost identical P-T-t paths (supporting information Figures Svi–Sviii), suggesting that a similar quantity and type of exhumed material is produced along the entire collision zone.

A number of the markers reach pressures and temperatures consistent with the production of HP/UHPM material (>2.7 GPa and >600°C) [*Chopin*, 1984]. The markers at the front of the continental block enter the subduction zone first and reach depths of >150 km (~4.5 GPa) and temperatures 800°C. Even markers that started 120 km from the front of the continental block reach depths of 50 km (~1.5 GPa) and temperatures of 200–400°C. A number of these rearward markers also return successfully to normal crustal levels. Some of the markers in the front of the continental block do not return completely to crustal levels, probably for two reasons: (1) limited exhumation of the whole subducted plate and (2), markers initially placed at 0–10 km depth partly accrete to the overriding plate during exhumation (Figure 3). At all depths there is a gradient in the peak pressures and temperatures achieved by markers (Figure 4), e.g., markers that are in the leading edge of the plate and enter the subduction zone first achieve much higher peak pressures and temperatures than markers further back from the front. The plate educts coherently, therefore, the pressure and temperature gradients defined by all markers are preserved in the educted material.

The P-T-t paths show that all the markers reach their peak pressure after ~20 Myr with an average initial burial rate of ~1–2 cm/yr followed by a slower phase of burial of ~0.5 cm/yr until the markers reach peak pressure (Figure 4). Exhumation rates are initially ~0.5 cm/yr but slow down even further as the material nears the surface. All the markers that successfully return to crustal depths do so within 40 Myr after their peak pressure and temperature was reached.

3.2. Diachronous Collision

The large-scale dynamics of a diachronous collision model are illustrated in Figure 5. The plate velocities are initially trench-perpendicular during oceanic plate subduction. Initial collision is in the "south" (Figure 5e) as a result of the promontory at the southern end of the incoming plate. Collision grades into continental subduction as this promontory slides beneath the overriding plate, and, consequently, subduction velocity reduces in the region of collision. In the meantime, collision and subduction continue to the "north" further along the collision zone, reaching the northern edge of the plate 18 Myr after initial collision (Figure 5f). The decrease in velocity at the point of initial collision causes a counter-clockwise rotation of the subducting plate with the pole of rotation starting below or to the south of the point of initial collision (i.e., outside our modeling domain at $y > 2640$ km), but then moves northward along the subduction zone as the point of collision progresses along the subduction zone (Figures 5e–5g).

Slab breakoff in this model starts at 22 Myr, under the region of the subduction zone that first experienced continental collision. A tear is created in the subducted oceanic slab at its contact with the continental leading edge (Animation S1 supporting information), which then propagates northward along the collisional zone until the full width of the oceanic slab (1980 km) detaches at 31 Myr. The breakoff results in a reversal in subduction velocity, starting in the area of initial collision in the south at 22 Myr (while subduction continues further along the subduction zone) and moving "northward" until the entire oceanic slab is detached at 31 Myr (Figure 5g).

The surface markers in each family are accreted onto the upper plate during continental subduction, as they are in the parallel collisional model. The deeper markers positioned initially at 10–30 km, however, are transported down along with the front portion of the continental plate (Figure 5). The southernmost markers experience the greatest amount of both burial and eduction compared to the other families of marker further along the collision zone (supporting information Figures Sx–Sxii). The continental plate subducts and exhumes coherently in the diachronous collision model (Figures 5a–5d). A comparison of Figures 5a–5d to Figures 3a–3d also shows that, in the area of initial collision, the diachronous collision model transports crustal material deeper (maximum depth of crustal material 220 km) than the orthogonal collision (maximum depth of crustal material 170 km).

The diachronous model also has the largest horizontal eduction distance of 174 km where collision was initiated, at the southern end of the collisional zone. Horizontal eduction distances decrease northward to 70 km in the center of the collision zone, and no eduction is recorded at all at the northern end of the collisional zone.

P-T-t paths for diachronous collision are presented in Figure 6 for the markers that start at 10–30 km depth and are from the family of markers positioned in the southern promontory of the subducting continental block ($y = 1980$ km). These markers lie at 0–120 km from the front of the continental block. P-T paths for all
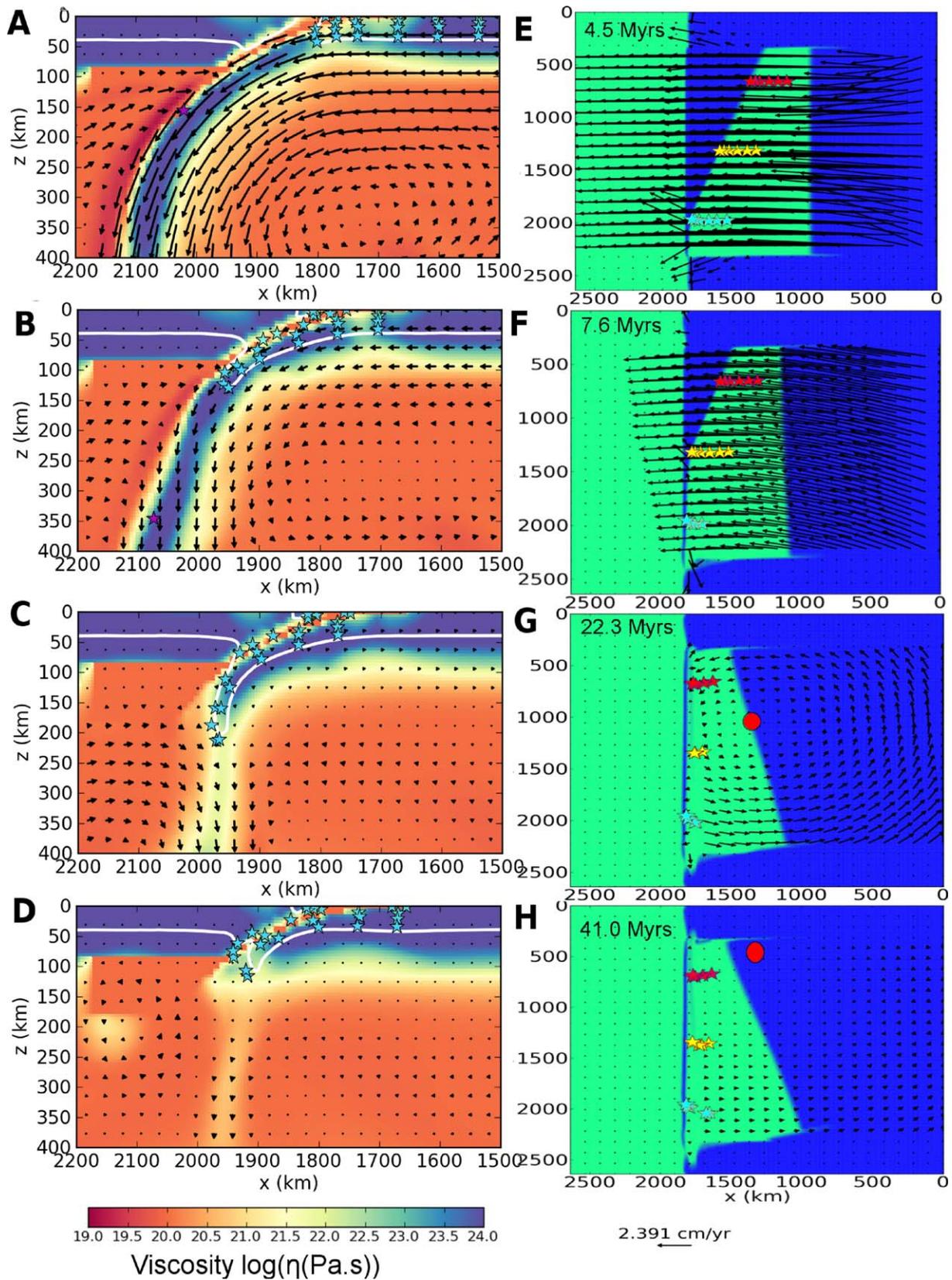
Figure 5. (a–d) Time slices through the diachronous collision model at the point where collision initiates. (e–h) Time snapshots of surface velocity. See Figure 3 for details. Red dot shows the position of the rotational pole.
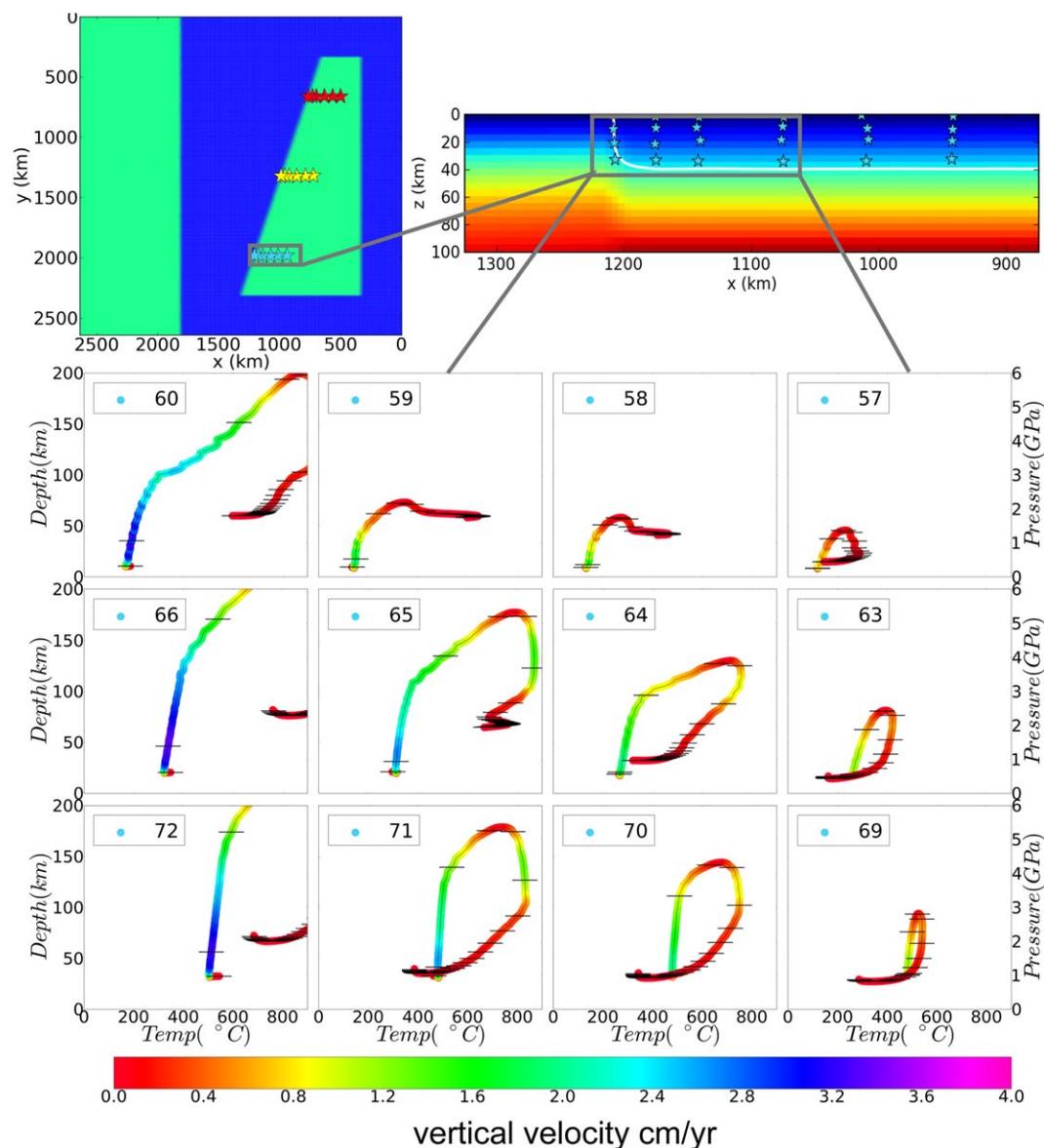
Figure 6. P-T-t (pressure-temperature-time) paths for material markers for diachronous collision that started at the southern promontory (y =1980 km) and were placed, from top to bottom, at 10, 20, and 30 km depth and, from left to right, at 0, 30, 60, and 120 km from the front of the subducting plate's continental block. The color of each P-T-t paths shows the vertical velocity of the material markers; the distances between the horizontal bars across the paths represent a passage of 5 Myr between bars.

three marker families are presented in the supporting information (Figures Sx–Sxii), which show that there are large along-trench variations in P-T paths, and that exhumation is much more likely in the region of initial collision than at the later, more northern, continental collision sites.

Markers closest to the front edge of the continental block reach depths of 200–250 km and temperatures of >900°C, though they only return to ∼60 km below the surface (Figure 6). However, a number of the markers that start further back from the edge of the continental block do return to crustal levels. For example, markers that start 30 km from the front of the continental block reach depths of 170 km (5 GPa) and temperatures of 850°C before returning to crustal levels (Figure 6). Even markers that start 120 km from the front of the continental block reach depths of 60–100 km and temperatures of 300–600°C (Figure 6). The difference in peak P-T conditions experienced by markers at the front edge of the plate and those further back from the edge produces a progressive metamorphic pattern toward the trench after the material is ultimately educted back to crustal depths.

BOTTRILL ET AL.   1776
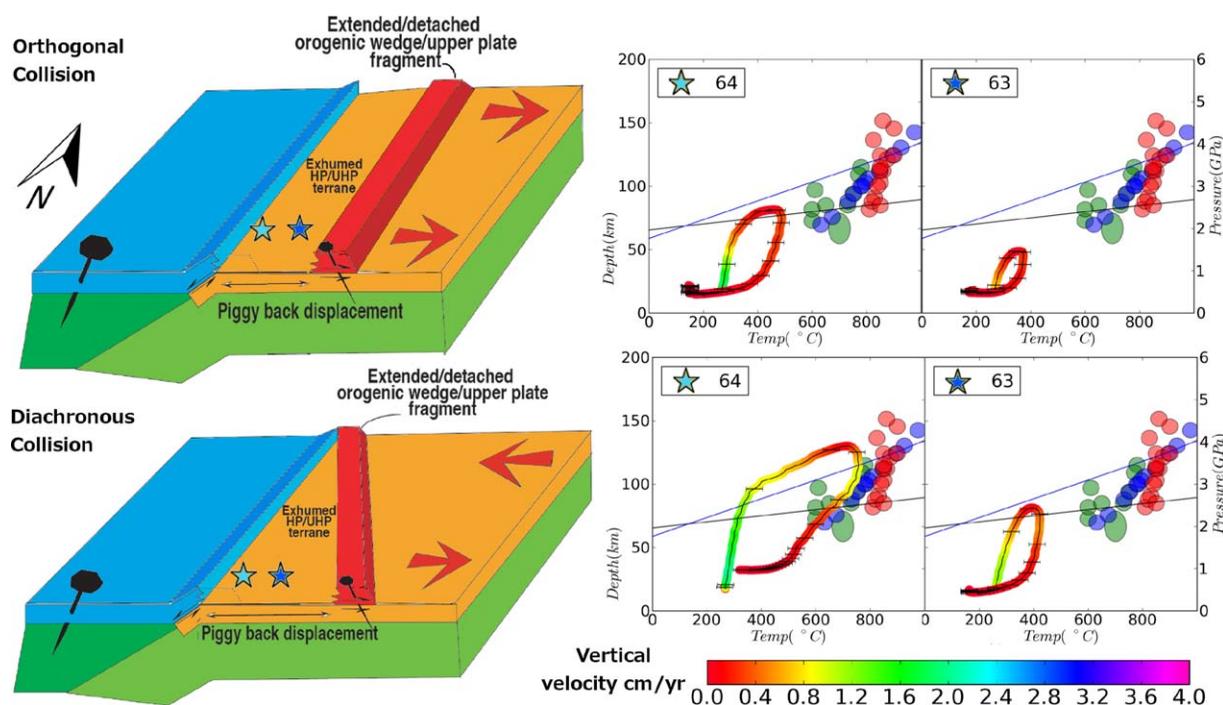
Figure 7. A schematic diagram of the exhumation dynamics for both the orthogonal and diachronous collision models [after Brueckner and Cuthbert, 2013]. The orthogonal collision model (top) subducts and educts uniformly all along the subduction zone whereas the diachronous collision model, (bottom) generates the greatest eduction distance at the southern end of the collision zone. This greater eduction distance is capable of passively transporting overlying allochthons shown in red) much further toward the foreland (bottom left) than would happen during orthogonal collision (top left). The P-T-t paths for identical tracers (start position, 20 km depth and 130 km (marker 64) and 190 km (marker 63) from the front edge of the continental block) both models are compared to petrological P-T estimates from the WGC, shown as ellipses [*Hacker et al.*, 2010] (green); [*Carswell et al.*, 2006] (red); [*Vrijmoed et al.*, 2006] (blue). These values are chosen to represent the deepest level of subduction in different regions of the WGC (see text for locations). We also show the diamond-graphite (blue line) [*Kennedy and Kennedy*, 1976] and coesite-quartz (black line) [*Bohlen and Boettcher*, 1982] stability fields. The P-T-t path for marker 64 shows that diachronous collision transports material 50 km deeper and to temperatures 300°C hotter than orthogonal collision and reaches the peak P-T data for the WGC whereas it does not in the orthogonal collision. The P-T-t path for marker 63 reaches the coesite transition during diachronous collision, but does not reach peak P-T conditions estimated for the WGC as it started 60 km further back from the front of the subducting plate and so was never subducted to the deepest levels of the WGC. This marker is analogous to the lower grade rock found in the interior of the WGC where eclogites were not generated.

The modeled P-T-t paths show that all the southernmost markers reach their peak pressure after ∼15 Myr with average burial rates that start at ∼1.5–3 cm/yr and then decline to a slower burial rate of 1–0.5 cm/yr until the markers reach their peak pressure (Figure 6). Exhumation rates are initially 0.5–1 cm/yr but slow down as the material nears the surface. All the markers that successfully return to crustal depths do so within 40 Myr after peak pressure and temperature were reached.

4. Discussion

The P-T-t loops that generate maximum P-T conditions in both the orthogonal and diachronous collision model are compared with published pressure and temperature estimates based on the geothermobarometry of eclogite facies assemblages that recrystallized within the WGC during Scandian subduction and early exhumation (Figure 7) [data from *Carswell et al.*, 2006; *Vrijmoed et al.*, 2006; *Hacker et al.*, 2010]. Some estimates from garnet peridotites are excluded because they may have formed while the peridotites were still in the mantle wedge, and not in the subducted continental crust.

It can be seen by inspection that the diachronous collisional model results in much higher P-T conditions (60 km deeper and 300°C hotter) than the orthogonal model and that the loop modeled for the most deeply subducted continental crust at the point of initial collision in the diachronous model successfully reaches the UHP stability fields of coesite and diamond. The loop also matches the pressure estimates from all of the P-T studies as well as the lower temperature estimates (600–800°C) from some of the studies. Some petrological temperature calculations are 50–100°C hotter than achieved by the loop, a difference not considered significant in view of the uncertainties in geothermobarometry [see discussions in *Ravna et al.*, 2004; *Cuthbert et al.*, 2004; *Carswell et al.*, 2006].

The published estimates for P-T paths followed by the WGC [e.g., *Labrousse et al.*, 2004] show "skinny" "hair-pin" shapes indicating that the large increase in pressure experienced by the eclogites was accompanied by a relatively small temperature change (<200°C). Our modeled P-T paths have "fatter" loops than the petrological estimates. This difference could imply that the modeled initial crustal temperature may have been hotter, or perhaps there was significant heating during the initial continental subduction. The diachronous collision model tends to create "skinnier hairpin" P-T paths by generating faster subduction and eduction, relative to the orthogonal model, thereby allowing material less time to equilibrate to mantle temperatures before and during its return to the surface. This can be seen by comparing Figures 4, 6, and 7 where the diachronous model shows slightly faster burial and exhumation rates. The degree to which a P-T loop is "skinny" or "fat" are likely to be related to the rate of subduction and exhumation. Very rapid rates for one or both of these processes should result in limited temperature increases as a result of the short time available for temperatures within the subducted slab to equilibrate with ambient mantle temperatures. The "skinny" loops in [*Labrousse et al.*, 2004] would imply relatively rapid subduction and eduction rates whereas the "fatter" loops generated by our models would allow for slower rates. Subduction rates are difficult to calculate, but exhumation rates have been estimated at 0.2–2.5 cm/yr [*Carswell et al.*, 2003; *Root et al.*, 2005]. These estimates, in turn, are strongly dependent on radiometric age determinations for the various steps in the subduction-exhumation process. The first dates generated from eclogites in the WGC gave ages from 440 to 400 Ma [*Griffin and Brueckner*, 1980], implying very slow subduction and/or exhumation. The older ages were challenged when more recent age determination gave more restricted ages closer to 400 Ma, implying the duration of subduction and exhumation was much shorter, on the order of 10 Myr [*Carswell et al.*, 2003; *Root et al.*, 2005]. However, still more recent publications have verified some of the older ages [*Spengler et al.*, 2006] leading to revised subduction/eduction cycles lasting as long as 35 Myr [*Kylander-Clark et al.*, 2012]. Therefore, given the uncertainties in both P-T calculations and age determinations, we propose that the P-T-t loops given, particularly by the diachronous model, are broadly consistent with the P-T-t history of the WGC.

The modeled P-T loops in Figure 7 broadly coincide with the cloud of published peak P-T estimates for the WGC. The data in Figure 7 came from a variety of locations [*Hacker et al.*, 2010], (green ellipsis) data are a compilation of estimates from several areas of the WGC while [*Carswell et al.*, 2006] (red ellipsis) present data from the islands of Fjørtoft and Otrøy in the most deeply subducted north west corner of the WGC. The [*Vrijmoed et al.*, 2006] data (blue ellipsis) are from a garnet peridotite on the west coast of Norway on the north-western edge of the WGC. This data represents the most deeply subducted material exhumed in the WGC. On the basis that the "peak" metamorphic paragenesis and mineral chemistry for a rock sample is frozen in at the pressure corresponding to the highest temperature in the P-T evolution it experienced [*Spear et al.*, 1984], the plotted P-T points in Figure 7 should approximately correspond to the start of the return segment of their P-T-t paths. However, the conversion of a dry eclogite protolith (gabbro, granulite) to eclogite requires water to drive the reactions [*Krabbendam et al.*, 2000]. This water may come from outside the eclogite or be produced inside by a dehydration reaction [*Konrad-Schmolke et al.*, 2008], but neither of these processes necessarily takes place at P for T_{max}, so it is possible that eclogite-facies assemblages can form during both prograde and retrograde metamorphism, as long as P-T conditions are in the eclogite-facies stability field. Given these considerations and the limitations inherent in present day available data, we conclude again that the modeled P-T paths give a reasonable approximation of the likely conditions achieved by the WGC.

Material nearer the leading edge of the subducted continental block in both models achieves higher peak P-T conditions than material further back into the continental block. This variation fits with observations from the WGC, as the eclogites of the WGC show increasing metamorphic grade from southeast to northwest (i.e., toward the Laurentia-Baltica suture zone) [*Hacker et al.*, 2010; *Brueckner and Cuthbert*, 2013]. The protoliths of the HP/UHP WGC rocks are mainly Middle Proterozoic (~1700–950 Myr) orthogneisses [*Tucker et al.*, 2004], and could well have been buried to midcrustal depths under younger sequences by the time of Paleozoic continental collision of Laurentia and Baltica. HP/UHP material from both models return to depths between 10 and 30 km, and later erosion and/or extension is likely to bring this material closer the surface. Several studies [*Carswell et al.*, 2003; *Labrousse et al.*, 2004; *Root et al.*, 2005] propose that the WGC experienced a reduction in exhumation rate after an initial phase of more rapid exhumation, possibly driven by later tectonic events, such as extension [*Fossen*, 1993, 2010].

The two different collision modes obviously result in very different spatial distribution patterns for where a HP/UHP terrane will ultimately return to the surface. The orthogonal collision zone exhumes material

uniformly along its entire length with an eduction distance of 156 km along its entire length whereas the diachronous collision model exhumes HP/UHP crustal material further (174 km) but only at one end of the collision zone, where the promontory that collided earliest was located. The Laurentia-Baltica collision only has one extensive Scandian (i.e., 430–390 Ma) HP/UHP terrane, the Western Gneiss Complex, near the southern end of the Scandinavian Caledonides. The diachronous collisional model was intentionally designed for initial collision to occur at the southern end of the collisional zone. This design is consistent with paleomagnetic plate motion reconstructions [*Torsvik et al.*, 1992; *Cocks and Torsvik*, 2002] that show how Baltica first collided with Laurentia at its southern tip and then collision migrated to the north. The plate reconstruction of *Torsvik et al.* [1992, 2012] also demonstrates that the south to north collision caused Baltica to rotate counter clockwise. Baltica's pole of rotation can be calculated, from the reconstruction [*Torsvik et al.*, 2012], (Figure Six and Animation S2 supporting information) for 15 Myr prior to Baltica and Laurentia locking together (430 Ma, in the reconstruction). Baltica's rotational pole moves north, roughly parallel to the collision zone, which is broadly consistent with the diachronous collisional model after initial collision of the continental promontory.

The amount of lateral exhumation predicted by both collision models provides additional support for the "piggyback" transport model of allochthons that rest tectonically on top of the WGC [*Rice*, 2005; *Brueckner and Cuthbert*, 2013]. Estimates for the lateral translations for some of these allochthons exceed 300 km [*Törnebohm*, 1896; *Gee*, 1975; *Hossack and Cooper*, 1986; *Gale et al.*, 1987]. Much of this displacement occurred by thrusting during the construction of the orogenic wedge associated with the initial collision of Baltica and Laurentia. However, a significant amount of the additional displacement may have been the result of "piggyback" transport on top of the WGC as it exhumed toward the east/southeast. Two of these allochthons, the Jotun and Trondheim Nappe Complexes, are estimated to have been carried a minimum distance of 30–60 km to their current position by this "piggyback" mechanism [*Brueckner and Cuthbert*, 2013], but much larger distances of 215–320 km have also been proposed [*Rice*, 2005]. The lower estimates fit with both models, which show horizontal eduction distances for the WGC of 156 km for orthogonal collision and 179 km for diachronous collision. If the allochthons began passive transport immediately after the initiation of eduction, half of their total displacement could be accounted for by the piggyback mechanism. The larger estimates of *Rice* [2005], however, are not consistent with the model.

Neither model reproduces all of the structural features that are typical of the WGC. For example, the Møre-Trøndelag Fault Zone bounds the WGC to the north and is a large high-angle shear zone with major left lateral displacement [*Fossen*, 2010]. The rather simple visco-plastic rheology in the model calculations and the absence of imposed preexisting faults, weak zones or other structures within the continental block precludes the formation of such structural features during the model runs. However, the Møre-Trøndelag Fault Zone could still fit the proposed diachronous collision and rotation model by acting as a vertical decollement that accommodated some of the differential movement between the north and south of Baltica during its collision with Laurentia. The surface boundary condition in the model is a nondeformable free slip boundary, which prevents the generation of actual topography in the model. The effect of a free slip boundary compared to a deformable boundary or the use of a sticky air layer has been summarized by *Schmeling et al.* [2008] and *Crameri et al.* [2012] for topography modeling. These studies conclude that although a true deformable surface is important, first order features are still reproduced with a simple nondeforming boundary. We therefore suggest that our models do capture the expected pattern of exhumed material and that a true free surface may actually assist in the eduction of material by providing less resistance to the bending of the subducted plate.

Finally, we briefly discuss the applicability of our results to other UHP terranes. In their recent review of ultrahigh-pressure tectonism, *Hacker and Gerya* [2013] summarized six different mechanisms for the exhumation of UHP rocks, of which eduction and microplate rotation were noted as two separate cases, with the rider that "There are, to date, no published analogue or computational models of UHP exhumation by microplate rotation." Our study supplies that model, and furthermore suggests that the rotation and eduction processes may be linked, with rotation enhancing the degree of eduction, and favoring both the deepest burial and greatest exhumation of continental crust. We therefore suggest that our results have relevance to UHP terranes where eduction and/or rotation have previously been proposed, including the Dabie Shan of China [*Wang et al.*, 2003] and eastern Papua New Guinea [*Webb et al.*, 2008]. It may also explain the exhumation process in regions where combined plate rotations and eduction have not been

proposed so far, such as the Dora Maira Massif of the Alps, where vertical axis rotations of the right age have been proposed [*Ford et al.*, 2006]. Additionally, our model may help explain why regional exposures of UHP rocks are rare in orogenic belts. If orthogonal collision produces lower degrees of burial, and, just as crucially, lower rates and amounts of exhumation, such collision zones will be less favorable sites for the generation and preservation of regional UHP terranes. We suggest that a future direction for research should be the evaluation of what amount, if any, of rotation and eduction is involved in the exhumation of each UHP region.

5. Conclusions

The diachronous collision and rotation of two colliding plates can assist in the eduction of material that has been transported to greater depths and experienced higher temperatures than would have been the case with an orthogonal collision. We also find that plate rotation exhumes material only in the area of initial collision, whereas an orthogonal collision exhumes material all along the subduction zone. Plate reconstructions for the Laurentia-Baltica collision suggest a diachronous collision mechanism and show a rotation of Baltica during its collision with Laurentia. Diachronous collision and the ensuing rotation of Baltica relative to Laurentia can explain the position of the WGC at the southern end of the Scandinavian Caledonides as the result of being the area of first collision. It also explains the extreme pressures and temperatures (4–5 GPa and 600–800°C) that generated eclogite in the most deeply subducted portions of the WGC since diachronous collision will drive crustal material deeper into the mantle than orthogonal collision, and makes it easier to exhume this deeply subducted material. Thus, rotation of the colliding Baltica plate may be important in explaining the subduction and exhumation of the WGC and potentially may be important for other extensive HP/UHP terranes both in terms of their positioning and experienced P-T-t evolution.

References

Andersen, T. B., and H. O. Austrheim (2008), The Caledonian infrastructure in the fjord region of western Norway: With special emphasis on formation and exhumation of high- and ultrahigh-pressure rocks, late- to post-orogenic tectonic processes and basin formation, in *33rd International Geological Congress*, pp. 1–88, Oslo.

Andersen, T. B., B. Jamtveit, J. F. Dewey, and E. Swensson (1991), Subduction and eduction of continental crust: Major mechanisms during continent-continent collision and orogenic extensional collapse, a model based on the south Norwegian Caledonides, *Terra Nova*, *3*, 303–310, doi:10.1111/j.1365-3121.1991.tb00148.x.

Andreasson, P. G., D. G. Gee, M. J. Whitehouse, and H. Schoberg (2003), Subduction-flip during Iapetus Ocean closure and Baltica-Laurentia collision, Scandinavian Caledonides, *Terra Nova*, *15*(6), 362–369, doi:10.1046/j.1365-3121.2003.00486.x.

Bohlen, S. R., and A. L. Boettcher (1982), Coesite transformation' of other components, *J. Geophys. Res.*, *87*(2), 7073–7078.

Bottrill, A. D., J. van Hunen, and M. B. Allen (2012), Insight into collision zone dynamics from topography: Numerical modelling results and observations, *Solid Earth*, *3*, 387–399, doi:10.5194/se-3-387-2012.

Brueckner, H. K. (2006), Dunk, dunkless and re-dunk tectonics: A model for metamorphism, lack of metamorphism, and repeated metamorphism of HP/UHP terranes, *Int. Geol. Rev.*, *48*, 978–995, doi:10.2747/0020-6814.48.11.978.

Brueckner, H. K., and S. J. Cuthbert (2013), Extension, disruption, and translation of an orogenic wedge by exhumation of large ultrahighpressure terranes: Examples from the Norwegian Caledonides, *Lithosphere*, *5*, 277–289, doi:10.1130/L256.1.

Brueckner, H. K., and H. L. M. van Roermund (2004), Dunk tectonics: A multiple subduction/eduction model for the evolution of the Scandinavian Caledonides, *Tectonics*, *23*, TC2004, doi:10.1029/2003TC001502.

Burov, E., L. Jolivet, L. Le Pourhiet, and A. Poliakov (2001), A thermomechanical model of exhumation of high pressure (HP) and ultra-high pressure (UHP) metamorphic rocks in Alpine-type collision belts, *Tectonophysics*, *342*, 113–136, doi:10.1016/S0040-1951(01)00158-5.

Butler, J. P., R. A. Jamieson, H. M. Steenkamp, and P. Robinson (2013), Discovery of coesite-eclogite from the Nordøyane UHP domain, Western Gneiss Region, Norway: Field relations, metamorphic history, and tectonic significance, *J. Metamorph. Geol.*, *31*, 147–163, doi: 10.1111/jmg.12004.

Byerlee, J. (1978), Friction of rocks, *Pure Appl. Geophys.*, *116*, 615–626.

Carswell, D. A., H. K. Brueckner, S. J. Cuthbert, K. Mehta, and P. J. O'Brien (2003), The timing of stabilisation and the exhumation rate for ultra-high pressure rocks in the Western Gneiss Region of Norway, *J. Metamorph. Geol.*, *21*, 601–612, doi:10.1046/j.1525-1314.2003.00467.x.

Carswell, D. A., H. L. M. van Roermund, and D. F. W. de Vries (2006), Scandian ultrahigh-pressure metamorphism of proterozoic basement rocks on Fjørtoft and Otrøy, Western Gneiss Region, Norway, *Int. Geol. Rev.*, *48*, 957–977, doi:10.2747/0020-6814.48.11.957.

Chopin, C. (1984), Coesite and pure pyrope in high-grade blueschists of the western Alps: A first record and some consequences, *Contrib. Mineral. Petrol.*, *86*, 107–118.

Cloos, M. (1993), Lithospheric buoyancy and collisional orogenesis: Subduction of oceanic plateaus, continental margins, island arcs, spreading ridges, and seamounts, *Geol. Soc. Am. Bull.*, *105*, 715, doi:10.1130/0016-7606.

Cocks, L. R. M., and T. H. Torsvik (2002), Earth geography from 500 to 400 million years ago: A faunal and palaeomagnetic review, *J. Geol. Soc. London*, *159*, 631–644.

Crameri, F., H. Schmeling, G. J. Golabek, T. Duretz, R. Orendt, S. J. H. Buiter, D. A. May, B. J. P. Kaus, T. V. Gerya, and P. J. Tackley (2012), A comparison of numerical surface topography calculations in geodynamic modelling: An evaluation of the "sticky air" method, *Geophys. J. Int.*, *189*(1), 38–54, doi:10.1111/j.1365-246X.2012.05388.x.

Cuthbert, S., D. Carswell, E. Krogh-Ravna, and A. Wain (2000), Eclogites and eclogites in the Western Gneiss Region, Norwegian Caledonides, *Lithos*, *52*, 165–195, doi:10.1016/S0024-4937(99)00090-0.

Cuthbert, S. J., M. A. Harvey, and D. A. Carswell (1983), A tectonic model for the metamorphic evolution of the Basal Gneiss Complex, Western South Norway, *J. Metamorph. Geol.*, *1*(1), 63–90, doi:10.1111/j.1525-1314.1983.tb00265.x.

Cuthbert, S. J., J. O. Buckman, and D. A. Carswell (2004), A crack-seal mechanism for deformation and compositional modification of eclogite garnets. *32nd International Geological Congress*, Florence, August 2004, *1*, abs. 153-12, p. 722.

Davies, J. H., and F. von Blanckenburg (1995), Slab breakoff: A model of lithosphere detachment and its test in the magmatism and deformation of collisional orogens, *Earth Planet. Sci. Lett.*, *129*(1–4), 85–102, doi:10.1016/0012-821X(94)00237-S.

Davies, N. S., P. Turner, and I. J. Sansom (2005), A revised stratigraphy for the Ringerike Group (Upper Silurian, Oslo Region), *Norw. J. Geol.*, *85*, 193–202.

Dewey, J. F., and R. A. Strachan (2003), Changing Silurian-Devonian relative plate motion in the Caledonides: Sinistral transpression to sinistral transtension, *J. Geol. Soc. London*, *160*(2), 219–229, doi:10.1144/0016-764902-085.

Di Giuseppe, E., J. van Hunen, F. Funiciello, C. Faccenna, and D. Giardini (2008), Slab stiffness control of trench motion: Insights from numerical models, *Geochem. Geophys. Geosyst.*, *9*, Q02014, doi:10.1029/2007GC001776.

Dixon, J. M., and E. Farrar (1980), Ridge subduction, eduction,and the Neogene Tectonics of southwestern North America, *Tectonophysics*, *67*, 81–99.

Dobrzhinetskaya, L., S. Faryad, and S. J. Cuthbert (2011a), Frontiers of ultrahigh pressure metamorphism: View from field and laboratory, in *Ultrahigh-Pressure Metamorphism: 25 Years After the Discovery of Coesite and Diamond*, edited by L. Dobrzhinetskaya, S. Faryad, S. Wallis, and S. J. Cuthbert, pp. 1–26, Elsevier Insights Ser., London.

Dobrzhinetskaya, L., S.-W. Faryad, S. Wallis, and S. Cuthbert (2011b), *Ultrahigh-Pressure Metamorphism: 25 Years After The Discovery Of Coesite and Diamond.*, Elsevier Insights Ser., London.

Dobrzhinetskaya, L. F., E. A. Eide, R. B. Larsen, B. A. Sturt, R. G. Trønnes, C. Smith, W. R. Taylor, and T. V. Posukhova (1995), Microdiamond in high-grade metamorphic rocks of the Western Gneiss region, Norway, *Geology*, *23*, 597–600, doi:10.1130/0091-7613.

Duretz, T., T. V. Gerya, B. J. P. Kaus, and T. B. Andersen (2012), Thermomechanical modeling of slab eduction, *J. Geophys. Res.*, *117*, B08411, doi:10.1029/2012JB009137.

Ford, M., S. Duchene, D. Gasquet, and O. Vanderhaeghe (2006), Two-phase orogenic convergence in the external and internal SW Alps, *J. Geol. Soc. London*, *163*, 815–826, doi:10.1144/0016-76492005-034.

Fossen, H. (1993), The role of extensional tectonics in the Caledonides of south Norway: Discussion, *J. Struct. Geol.*, *15*, 1379–1380.

Fossen, H. (2010), Extensional tectonics in the North Atlantic Caledonides: A regional view, *Geol. Soc. London*, *335*(1), 767–793, doi:10.1144/SP335.31.

Gale, R., A. H. N. Rice, D. Roberts, C. Townsend, and A. Welbon (1987), Restoration of the Baltoscandian Caledonian margin from balanced cross sections: The problem of excess continental crust, *Trans. R. Soc. Edinburgh Earth Sci.*, *78*, 197–217.

Gee, D. G. (1975), A tectonic model for the central part of the Scandinavian Caledonides, *Am. J. Sci.*, *275*, 468–515.

Gee, D. G., C. Juhlin, C. Pascal, and P. Robinson (2010), Collisional Orogeny in the Scandinavian Caledonides (COSC), *GFF*, *132*, 29–44, doi:10.1080/11035891003759188.

Glodny, J., A. Kühn, and H. Austrheim (2008), Geochronology of fluid-induced eclogite and amphibolite facies metamorphic reactions in a subduction–collision system, Bergen Arcs, Norway, *Contrib. Mineral. Petrol.*, *156*, 27–48, doi:10.1007/s00410-007-0272-y.

Griffin, W., G. Austrheim, K. Brastad, I. Brynhi, A. Krill, J. Krogh, J. Mork, M. Qvale, and B. Torudbakken (1985), *High Pressure Metamorphism in the Scandinavian Caledonides*, edited by D. G. Gee and B. A. Sturt, The Caledonian orogen—Scandinavia and related areas, pp. 783–801, John Wiley, New York.

Griffin, W. L., and H. K. Brueckner (1980), Caledonian Sm–Nd ages and a crustal origin for Norwegian eclogites, *Nature*, *285*(5763), 319–321, doi:10.1038/285319a0.

Hacker, B. R. (2007), Ascent of the ultrahigh-pressure Western Gneiss Region, Norway, *Spec. Pap. Geol. Soc. Am.*, *2419*(4), 171–184, doi:10.1130/2006.2419(09).

Hacker, B. R., and P. B. Gans (2005), Continental collisions and the creation of ultrahigh-pressure terranes: Petrology and thermochronology of nappes in the central Scandinavian Caledonides, *Geol. Soc. Am. Bull.*, *117*(1), 117–134, doi:10.1130/B25549.1.

Hacker, B. R., and T. V. Gerya (2013), Paradigms, new and old, for ultrahigh-pressure tectonism, *Tectonophysics*, *603*, 79–88, doi:10.1016/j.tecto.2013.05.026.

Hacker, B. R., T. B. Andersen, D. B. Root, L. Mehl, J. M. Mattinson, and J. L. Wooden (2003), Exhumation of high-pressure rocks beneath the Solund Basin, Western Gneiss Region of Norway, *J. Metamorph. Geol.*, *21*, 613–629, doi:10.1046/j.1525-1314.2003.00468.x.

Hacker, B. R., T. B. Andersen, S. Johnston, A. R. C. Kylander-Clark, E. M. Peterman, E. O. Walsh, and D. Young (2010), High-temperature deformation during continental-margin subduction & exhumation: The ultrahigh-pressure Western Gneiss Region of Norway, *Tectonophysics*, *480*, 149–171, doi:10.1016/j.tecto.2009.08.012.

Hossack, J. R., and M. A. Cooper (1986), Collision tectonics in the Scandinavian Caledonides, in *Collision tectonics: Geological Society of London Special Publication*, edited by M. P. Coward and A. C. Ries, pp. 287–304, GSL, London.

Karato, S.-I., and P. Wu (1993), Rheology of the upper mantle: A synthesis., *Science*, *260*, 771–778, doi:10.1126/science.260.5109.771.

Kennedy, C. S., and G. C. Kennedy (1976), The equilibrium boundary between graphite and diamond, *J. Geophys. Res.*, *81*(14), 2467–2470.

Konrad-Schmolke, M., P. J. O'Brien, C. de Capitani, and D. A. Carswell (2008), Garnet growth at high- and ultra-high pressure conditions and the effect of element fractionation on mineral modes and composition, *Lithos*, *103*, 309–332, doi:10.1016/j.lithos.2007.10.007.

Krabbendam, M., A. Wain, and T. B. Andersen (2000), Pre-Caledonian granulite and gabbro enclaves in the Western Gneiss Region, Norway: Indications of incomplete transition at high pressure, *Geol. Mag.*, *137*, 235–255, doi:10.1017/S0016756800004015.

Krogh, E. J. (1977), Evidence of Precambrian continent–continent collision in Western Norway, *Nature*, *267*, 17–19, doi:10.1038/267017a0.

Krogh Ravna, E. J., and M. P. Terry (2004), Geothermobarometry of UHP and HP eclogites and schists–an evaluation of equilibria among garnet-clinopyroxene-kyanite-phengite-coesite/quartz, *J. Metamorph. Geol.*, *22*, 579–592, doi:10.1111/j.1525-1314.2004.00534.x.

Kylander-Clark, A. R. C., B. R. Hacker, C. Johnson, B. Beard, N. Mahlen, and T. Lapen (2007), Coupled Lu–Hf and Sm–Nd geochronology constrains prograde and exhumation histories of high- and ultrahigh-pressure eclogites from western Norway, *Chem. Geol.*, *242*, 137–154, doi:10.1016/j.chemgeo.2007.03.006.

Kylander-Clark, A. R. C., B. R. Hacker, C. M. Johnson, B. L. Beard, and N. J. Mahlen (2009), Slow subduction of a thick ultrahigh-pressure terrane, *Tectonics*, *28*, TC2003, doi:10.1029/2007TC002251.

Kylander-Clark, A. R. C., B. R. Hacker, and C. G. Mattinson (2012), Size and exhumation rate of ultrahigh-pressure terranes linked to orogenic stage, *Earth Planet. Sci. Lett.*, *321–322*, 115–120, doi:10.1016/j.epsl.2011.12.036.

Labrousse, L., L. Jolivet, T. B. Andersen, P. Agard, R. Hébert, H. Maluski, and U. Schärer (2004), Pressure-temperature-time deformation history of the exhumation of ultra-high pressure rocks in the Western Gneiss Region, Norway, *Spec. Pap. Geol. Soc. Am.*, *380*, 155–183.

Milnes, A. G., and F. Corfu (2008), Structural geology and tectonic evolution of the Sognefjord transect, Caledonian orogen, southern Norway, in *paper presented at 33rd International Geological Congress*, pp. 1–94, Oslo.

Moresi, L., and M. Gurnis (1996), Constraints on the lateral strength of slabs from three-dimensional dynamic flow models, *Earth Planet. Sci. Lett.*, *138*, 15–28, doi:10.1016/0012-821X(95)00221-W.

Nolet, G. (2009), Slabs do not go gently, *Science*, *324*, 1152–1153.

Rice, A. H. N. (2005), Quantifying the exhumation of UHP-rocks in the Western Gneiss region, S. W. Norway: A branch-line–balanced cross-section model, *Aust. J. Earth Sci.*, *98*, 2–21.

Robinson, P. (1995), Extension of Trollheimen tectono-stratigraphic sequence in deep synclines near Molde and Brattvåg, Western Gneiss Region, southern Norway., *Nor. Geol. Tidsskr.*, *75*, 181–198.

Roecker, S. W. (1982), Velocity structure of the Pamir–Hindu Kush region: Possible evidence of subducted crust, *J. Geophys. Res.*, *87*(B2), 945–959.

Root, D. B., B. R. Hacker, P. B. Gans, M. N. Ducea, E. A. Eide, and J. L. Mosenfelder (2005), Discrete ultrahigh-pressure domains in the Western Gneiss Region, Norway: Implications for formation and exhumation, *J. Metamorph. Geol.*, *23*(1), 45–61, doi:10.1111/j.1525-1314.2005.00561.x.

Schmeling, H., et al. (2008), A benchmark comparison of spontaneous subduction models—Towards a free surface, *Phys. Earth Planet. Inter.*, *171*(1–4), 198–223, doi:10.1016/j.pepi.2008.06.028.

Smith, D. C. (1984), Coesite in clinopyroxene in the Caledonides and its implications for geodynamics, *Nature*, *310*, 641–644, doi:10.1038/310641a0.

Spear, F. S., J. Selverstone, D. Hickmott, P. Crowley, and K. V. Hodges (1984), P-T paths from garnet zoning: A new technique for deciphering tectonic processes in crystalline terranes, *Geology*, *12*(2), 87–90, doi:10.1130/0091-7613(1984)12.

Spengler, D., H. L. M. van Roermund, M. R. Drury, L. Ottolini, P. R. D. Mason, and G. R. Davies (2006), Deep origin and hot melting of an Archaean orogenic peridotite massif in Norway, *Nature*, *440*(7086), 913–917, doi:10.1038/nature04644.

Spengler, D., H. K. Brueckner, H. L. M. van Roermund, M. R. Drury, and P. R. D. Mason (2009), Long-lived, cold burial of Baltica to 200 km depth, *Earth Planet. Sci. Lett.*, *281*, 27–35, doi:10.1016/j.epsl.2009.02.001.

Sperner, B., F. Lorenz, K. Bonjer, S. Hettel, R. D. Müller, F. Wenzel, and B. Mu (2001), Slab break-off ± abrupt cut or gradual detachment? New insights from the Vrancea Region (SE Carpathians, Romania), *Terra Nova*, *13*(3), 172–179.

Terry, M. P., P. Robinson, and E. J. K. Ravna (2000), Kyanite eclogite thermobarometry and evidence for thrusting of UHP over HP metamorphic rocks, Nordøyane, Western Gneiss Region, Norway, *Am. Mineral.*, *85*, 1637–1650.

Teyssier, C. (2011), Exhumation of deep orogenic crust, *Lithosphere*, *3*, 439–443, doi:10.1130/RF.L002.1.

Törnebohm, A. E. (1896), Grunddragen af det Centrala Skan-dinavians Bergbyggnad, *Sven. Vetenskap-Sakademiens Handl.*, *2*, 1–210.

Torsvik, T. H., M. A. Smethurst, R. Van der Voo, A. Trench, N. Abrahamsen, and E. Halvorsen (1992), Baltica: A synopsis of vendian-permian palaeomagnetic data and their palaeotectonic implications, *Earth Sci. Rev.*, *33*(2), 133–152, doi:10.1016/0012-8252(92)90023-M.

Torsvik, T. H., et al. (2012), Phanerozoic polar wander, palaeogeography and dynamics, *Earth Sci. Rev.*, *114*, 325–368, doi:10.1016/j.earscirev.2012.06.007.

Tucker, R. D., P. Robinson, A. Solli, D. G. Gee, T. Thorsnes, T. E. Krogh, Ø. Nordgulen, and M. E. Bickford (2004), Thrusting and extension in the Scandian Hinterland, Norway: New U-Pb ages and tectonostratigraphic evidence, *Am. J. Sci.*, *304*(June), 477–532.

Van der Meulen, M. J., J. E. Meulenkamp, and R. Wortel (1998), Lateral shifts of Apenninic foredeep depocentres reflecting detachment of subducted lithosphere, *Earth Planet. Sci. Lett.*, *154*(1–4), 203–219, doi:10.1016/S0012-821X(97)00166-0.

Van Hunen, J., and M. B. Allen (2011), Continental collision and slab break-off: A comparison of 3-D numerical models with observations, *Earth Planet. Sci. Lett.*, *302*, 27–37, doi:10.1016/j.epsl.2010.11.035.

Van Roermund, H. L. M., D. A. Carswell, M. R. Drury, T. C. Heijboer, and H. L. M. Van Roermund (2002), Microdiamonds in a megacrystic garnet websterite pod from Bardane on the island of Fjortoft, western Norway: Evidence for diamond formation in mantle rocks during deep continental subduction, *Geology*, *30*, 957–1052, doi:10.1130/0091-7613(2002)030<0959.

Vrijmoed, J. C., H. L. M. Van Roermund, and G. R. Davies (2006), Evidence for diamond-grade ultra-high pressure metamorphism and fluid interaction in the Svartberget Fe–Ti garnet peridotite–websterite body, Western Gneiss Region, Norway, *Mineral. Petrol.*, *88*(1–2), 381–405, doi:10.1007/s00710-006-0160-6.

Wain, A. (1997), New evidence for coesite in eclogite and gneisses: Defining an ultrahigh-pressure province in the Western Gneiss region of Norway, *Geology*, *25*, 927–930, doi:10.1130/0091-7613(1997)025<0927.

Walsh, E. O., and B. R. Hacker (2004), The fate of subducted continental margins: Two-stage exhumation of the high-pressure to ultrahigh-pressure Western Gneiss Region, Norway, *J. Metamorph. Geol.*, *22*, 671–687, doi:10.1111/j.1525-1314.2004.00541.x.

Walsh, E. O., B. R. Hacker, P. B. Gans, M. S. Wong, and T. B. Andersen (2013), Crustal exhumation of the Western Gneiss Region UHP terrane, Norway: 40Ar/39Ar thermochronology and fault-slip analysis, *Tectonophysics*, *608*, 1159–1179, doi:10.1016/j.tecto.2013.06.030.

Wang, E., Q. Meng, B. C. Burchfiel, and G. Zhang (2003), Mesozoic large-scale lateral extrusion, rotation, and uplift of the Tongbai–Dabie Shan belt in east China, *Geology*, *31*, 307–310, doi:10.1130/0091-7613(2003)031<0307.

Warren, C. J. (2013), Exhumation of (ultra-)high-pressure terranes: Concepts and mechanisms, *Solid Earth*, *4*, 75–92, doi:10.5194/se-4-75-2013.

Warren, C. J., C. Beaumont, and R. A. Jamieson (2008a), Formation and exhumation of ultra-high-pressure rocks during continental collision: Role of detachment in the subduction channel, *Geochem. Geophys. Geosyst.*, *9*, Q04019, doi:10.1029/2007GC001839.

Warren, C. J., C. Beaumont, and R. A. Jamieson (2008b), Modelling tectonic styles and ultra-high pressure (UHP) rock exhumation during the transition from oceanic subduction to continental collision, *Earth Planet. Sci. Lett.*, *267*, 129–145, doi:10.1016/j.epsl.2007.11.025.

Webb, L. E., S. L. Baldwin, T. A. Little, and P. G. Fitzgerald (2008), Can microplate rotation drive subduction inversion, *Geology*, *36*, 823, doi:10.1130/G25134A.1.

Wilks, W. J., and S. J. Cuthbert (1994), The evolution of the Hornelen Basin detachment system, western Norway: Implications for the style of late orogenic extension in the southern Scandinavian Caledonides, *Tectonophysics*, *238*, 1–30.

Wortel, M. J. R., and W. Spakman (2000), Subduction and slab detachment in the Meditaranian-Carpathian region, *Science*, *290*(December), 1910–1917, doi:10.1126/science.290.5498.1910.

Yoshioka, S., M. J. R. Wortel, and R. Wortel (1995), Three-dimensional numerical modeling of detachment of subducted lithosphere, *J. Geophys. Res.*, *100*(94), 20,223–20,244.

Zhang, R. Y., J. G. Liou, and W. G. Ernst (2009), The Dabie–Sulu continental collision zone: A comprehensive review, *Gondwana Res.*, *16*, 1–26, doi:10.1016/j.gr.2009.03.008.

Zhong, S., M. T. Zuber, L. Moresi, and M. Gurnis (2000), Role of temperature-dependent viscosity and surface plates in spherical shell models of mantle convection, *J. Geophys. Res.*, *105*(B5), 11,063–11,082.